

TRITA-PFU-91-03

**PARAMAGNETISM AND PLASMA BETA
IN A SCREW-PINCH**

B. Lehnert and J. Scheffel

TRITA-PFU-91-03

**PARAMAGNETISM AND PLASMA BETA
IN A SCREW-PINCH**

B. Lehnert and J. Scheffel

Stockholm, February 1991

Department of Plasma Physics and Fusion Research
Alfvén Laboratory, Royal Institute of Technology
S-100 44 Stockholm, Sweden

PARAMAGNETISM AND PLASMA BETA IN A SCREW-PINCH

B. Lehnert and J. Scheffel

*Department of Plasma Physics and Fusion Research
Alfvén Laboratory, Royal Institute of Technology, S - 100 44 Stockholm, Sweden*

Abstract

Anisotropic resistivity causes paramagnetic effects ($B_z'(r) < 0$) in a screw pinch, being basically different to the self-relaxation described by Taylor. We compute, analytically and numerically, the resulting effect on equilibrium in a 1-D straight cylindrical plasma. In particular we compute paramagnetic effects on the plasma radius and on plasma beta. Ohm's law also contains diamagnetic terms; in this paper we consider radial particle diffusion and the Nemst effect. In a Tokamak or reactor plasma these effects are shown to be negligible, whereas they may contribute in present ULQ, Extrap and RFP experiments.

A basic result is an expression for the coupling between the poloidal and axial magnetic field components with the above effects included. A result of specific importance to the Extrap programme is that plasma current limitation can arise from lack of equilibrium when the plasma radius tends to exceed its upper limit, being defined by a magnetic or material limiter. The paramagnetic effect described in this work lowers the plasma beta further, making D-D reactors depending on safety factors $q(a) > 1$ seem less attainable.

1. INTRODUCTION

In a magnetized plasma with a helical field structure, anisotropic resistivity will have a tendency to channel the current density pattern along the screw-shaped magnetic field lines. This paper presents investigations on stationary, however non-static, equilibria of such states in a cylindrical plasma column, where the anisotropic resistivity produces a coupling between the transverse (poloidal) and axial (toroidal) current and magnetic field components.

It is well known that anisotropic resistivity causes a paramagnetic effect, i.e. the axial magnetic field of a screw pinch will fall off with increasing radius. In this paper we will also show that the plasma radius itself is a function of the externally applied axial field, and compute the radius for various configurations. We use the generalized Ohm's law, also including the Nernst effect [1,2] and radial diffusion of particles. The latter effect can become important when the plasma is surrounded by a partially ionized boundary layer and a penetrating neutral gas, introducing sources of ions inside the plasma boundary. The result is a diffusion-driven current, which fortunately acts so as to enhance the total plasma current. In Z-pinch configurations (no axial magnetic field), paramagnetism due to anisotropic resistivity cannot appear, whereas the diffusion driven diamagnetic current may still be substantial.

Reversed field pinches (RFP) have relaxed states of dynamical equilibrium, due to the dynamo mechanism which couples the poloidal and toroidal field components [3]. The effect due to anisotropic resistivity considered in this paper is a quite different mechanism for the coupling of field components. Recent results indicate that the self-relaxation mechanism becomes suppressed in Extrap geometries due to the presence of the octupole field, which acts as poloidal divertor. Further, the poloidal field in Extrap is stronger both than that predicted by the Taylor Bessel function model and that achieved in RFP experiments [3,4].

In fusion research on alternative lines, a desirable goal is to minimize the axial magnetic field, or even to get rid of it, in order to obtain a high plasma beta-value. In a number of Z-pinch experiments in the Extrap configuration, efforts have been made to obtain high, confined plasma currents in the absence of an axial magnetic field [5]. In modest geometries (the linear device Extrap-L1), currents confined inside the separatrix of only about 5 kA have been obtained for a plasma radius $a = 0.02$ m [6]. The scaling of current to radial dimensions is not yet fully investigated, neither theoretically nor experimentally, and it is still unknown whether reactor relevant parameters may become attainable in the Extrap configuration, without using axial magnetic field. This current limitation can be due to lack of equilibrium, i.e. the plasma pressure is so low that the pinch radius tends to exceed the radius of the magnetic or material limiter. We argue here, that the same mechanism can be active in the presence of an axial magnetic field. In this case one also has to consider that the edge safety factor has to be sufficiently large.

2. BASIC EQUATIONS AND ASSUMPTIONS

A linear Z-pinch with circular cross-section is assumed to be sustained in an equilibrium state by an applied axial electric field $E_0 = \text{const}$. The stability of the pinch will not be discussed in this context. Radial plasma profiles are the electron density $n(r)$, the ion and electron temperatures $T(r)$, and the pressure $p(r) = 2nkT$. Introducing cylindrical coordinates (r, ϕ, z) , with z along the pinch axis, the starting points of the present analysis are as follows:

- There is a fully ionised plasma core in the region $0 < r \leq a$. Outside the core radius $r = a$ there is a partially ionized boundary layer. Within the latter, the plasma - neutral gas recirculation generates diffusion driven bootstrap-like currents.

- The electric field is given by $\mathbf{E} = (E_r, 0, E_z)$, the magnetic field $\mathbf{B} = (0, B_\phi, B_z)$ and the current density $\mathbf{j} = (0, j_\phi, j_z)$. The axial magnetic field at the core radius is denoted by $B_{za} = B_z(a)$. It becomes equal to an externally imposed axial field when the contribution from the diffusion driven current in the boundary layer can be neglected. The poloidal field B_ϕ is basically the plasma self-field; other contributions are neglected here.

- The resistivity tensor η is anisotropic and its components parallel and perpendicular to \mathbf{B} are denoted by $\eta_{//}$, and $\eta_{\perp} \equiv \eta = f\eta_{//}$, respectively. Classical Spitzer resistivity is given by $\eta = 129 (Z \ln \Lambda) / T^{3/2}$ with T in K, and by $f = 1.97$. In our numerical calculations we will, however, use the Braginskii value (see also Ref[7])

$$f = 1.97 \frac{x^4 + 8.38x^2 + 1.93}{x^4 + 14.8x^2 + 3.77}, \quad x = \omega_{ce} \tau_e$$

where $\omega_{ce} \tau_e = 5.8 \cdot 10^{22} B T^{3/2} [\text{eV}] / (n \ln \Lambda)$ is the product between the electron cyclotron frequency and collision time. This expression for f is also valid for weak magnetic fields (high collisionality).

Using SI-units and conventional symbols, the relevant basic equations become

$$\nabla \times \mathbf{B} = \mu_0 \mathbf{j} \quad (1)$$

$$\rho(\mathbf{v} \cdot \nabla) \mathbf{v} = \mathbf{j} \times \mathbf{B} - \nabla p \quad (2)$$

$$\mathbf{E} + \mathbf{v} \times \mathbf{B} = \frac{1}{ne} [\mathbf{j} \times \mathbf{B} - \nabla p_e] + \eta \mathbf{j} - \beta_{\perp} \nabla_{\perp} T_e - \beta_{\parallel} (\mathbf{h} \times \nabla T_e) \quad (3)$$

$$\eta_{ik} = \eta_{\perp} \delta_{ik} + (\eta_{//} - \eta_{\perp}) h_i h_k \quad (4)$$

We use the notation $\mathbf{n} \equiv \mathbf{B}/B$, where $B = |\mathbf{B}|$. The classical Braginskii transport coefficients are used in Ohm's law.

The present assumptions represent a first, simplified model of resistive and diffusive plasma equilibrium in a quasi-stable Z- or screw pinch. It should also apply to linear and large aspect ratio toroidal Extrap discharges, provided that effects due to deviation from a circular cross-section can be neglected. We emphasize that in this paper transverse and axial field components are coupled through anisotropic resistivity and radial diffusion, not by the Taylor dynamo mechanism.

3. THE EQUILIBRIUM STATE

The radial component of Eq. (3) yields

$$E_r + v_\phi B_z - v_z B_\phi = \frac{1}{ne} \left[j_\phi B_z - j_z B_\phi - \frac{p'}{2} \right] - \frac{\beta_\perp}{ne} T_e' \quad (5)$$

We denote the radial derivative by a prime (') and use $\partial/\partial\phi = \partial/\partial z = 0$. The electron pressure is assumed to equal half the total kinetic pressure. Eq. (5) determines the ambipolar electric field, basically due to the pressure gradient. We will not need to discuss Eq.(5) further here.

The azimuthal and axial components of Eq.(3) becomes

$$\eta \left[\left(1 + \frac{1-f}{f} h_\phi^2 \right) j_\phi + \frac{1-f}{f} h_\phi h_z j_z \right] = h_z \beta_\perp^* T_e' - v_r B_r \quad (6)$$

$$\eta \left[\frac{1-f}{f} h_\phi h_z j_\phi + \left(1 + \frac{1-f}{f} h_z^2 \right) j_z \right] = E_0 - h_\phi \beta_\perp^* T_e' + v_r B_\phi \quad (7)$$

in which equations the coupling between the magnetic field and current components become obvious. We have assumed $E_\phi = 0$. Also, $E_z(r) = E_0 = \text{constant}$, since $\nabla \times \mathbf{E} = \mathbf{0}$. Further, for singly charged ions

$$\beta_\perp^* = \frac{x(1.5x^2 + 3.1)}{e(x^4 + 14.8x^2 + 3.77)} \quad , \quad x \equiv \omega_{ce} \tau_e \quad (8)$$

After elimination of the currents in Eqs. (1), (6) and (7), the following simple differential equation is obtained ($E_0 B_\phi > 0$):

$$B_z' + \frac{(rB_\phi)'}{r} \frac{(f-1)B_\phi E_0 + B(\beta_\perp^* T_e' - Bv_r)}{(fB_z^2 + B_\phi^2)E_0 - B_\phi B(\beta_\perp^* T_e' - Bv_r)} B_z = 0 \quad (9)$$

This is the basic relation of our paper. It reveals that resistivity anisotropy ($f > 1$) is paramagnetic to its nature ($B_z' < 0$), and that the Nemst effect and velocity diffusion due to ion sources ($v_r > 0$) have an opposite, diamagnetic effect. Note also that the paramagnetic effect is independent of η , the magnitude of the resistivity. Hence Eq.(9) may apply even if resistivity is anomalous, which unfortunately usually is the case. The question is now: what is the influence of the 'non-ideal' terms corresponding to the Nemst effect and radial diffusion?

3.1 The Nernst effect

From Eq.(9) above one obtains the ratio of the Nernst term to 'ideal' terms as

$$\left| \frac{B\beta^*T}{(f-1)B_\phi E_0} \right| = 1.7 \cdot 10^{-23} \frac{n \ln \Lambda}{B_\phi E_0 L_T \sqrt{T}} \quad (10)$$

where L_T is the local scale length of the temperature profile. Way off the plasma boundary, this ratio is negligible. In present Extrap-T1 experiments (parameters; see Fig.3 b)) the above ratio is of order 0.1 near the boundary, whereas JET parameters give a ratio of order 0.001. Generally, the Nernst term can be neglected for sufficiently high edge temperatures T and low densities n , according to Eq.(10).

In our numerical calculations in Section 6 we always include the Nernst term in Eq.(9).

3.2 Radial particle diffusion

The radial diffusion of ions is extremely difficult to model. From the continuity equation we readily obtain

$$v_r(r) = \frac{1}{m(r)} \int_0^r r q_s(r) dr \quad (11)$$

where the source rate $q_s = n n_n \langle \sigma w \rangle_{ei} m^{-3} s^{-1}$, with n denoting ion density, n_n is the neutral gas density, and $\langle \sigma w \rangle_{ei}$ is the electron ionization rate of neutrals. Again we are dealing with a non-ideal effect which can only be significant near the boundary of a sufficiently dense plasma, with a core being impermeable to neutrals. Considering that the ionization rate is very sensitively depending on temperature, the profile of which itself is sensitive to boundary conditions, it becomes apparent that a proper model necessarily has to be self-consistent near the boundary.

The present study will not extend as far as to self-consistent modelling of edge transport. Our main interest is rather to determine whether the current caused by radial particle diffusion[5] can have any profound diamagnetic effect. It is clear from Eq.(7) that this 'bootstrap-like' current enhances the externally imposed electric field and thereby the total current. We will estimate q_s as follows.

The plasma-neutral gas boundary layer is a narrow region in which the electron density has a relatively slow radial dependence in comparison with that of the neutral gas. An upper limit for the neutral gas density is the filling density, given by $n_{\text{fill}} = 3.30 \cdot 10^{19} p_{\text{fill}} [\text{mTorr}]$; p_{fill} is the filling pressure. For boundary temperatures below 10 eV, $\langle \sigma w \rangle_{ei} \leq 10^{-14} \text{ m}^3 \text{ s}^{-1}$. Hence a true over-estimate of q_s would be obtained by using the latter value together with electron and neutral densities equal to the filling density. A filling pressure of 20 mTorr then yields $q_s = 4 \cdot 10^{27} \text{ m}^{-3} \text{ s}^{-1}$ in the boundary region. Experimental values of q_s are expected to be far lower.

In our numerical Section we will find that source rates of this caliber have strong diamagnetic effects. We will use more realistic values, and we will assume $q_s(r)$ to have the constant value q_0 over the entire plasma cross-section, motivated by that although the neutral density increases in the radial direction, $\langle \sigma w \rangle_{ei}$ steeply falls off. The real distribution of $q_s(r)$ is determined by the quasi-steady plasma-neutral gas balance in the boundary layer[5].

Finally we estimate the source rate necessary to produce an appreciable diffusion-driven current from Eq.(9). The ratio

$$\left| \frac{B^2 v_r}{(f-1) B_\phi E_0} \right| = \frac{r B^2}{2 B_\phi n E_0} q_0 \quad (12)$$

is obtained with the aid of Eq.(11). Using typical values for the Extrap experiment, the ratio at the boundary becomes of order $10^{-24} q_0$. Apparently we cannot rule out the possibility that a largely contributing diamagnetic current is generated.

3.3 Isotropic resistivity

Plasma resistivity is commonly assumed to be isotropic. This is in general not true, so it becomes of interest to find out under what exceptional circumstances isotropicity holds.

Using the approximate value $f=2$, the following relation is obtained from Eq.(3) by writing $\mathbf{j} = \mathbf{j}_\perp + \mathbf{j}_\parallel$ and using $\mathbf{j}_\perp = \mathbf{B} \times \nabla p / B^2$ (we neglect radial diffusion and assume $\omega_{ce} \tau_e \gg 1$):

$$\mathbf{E} = \frac{1}{ne} [\mathbf{j} \times \mathbf{B} - \nabla p_e] + \frac{1}{2} \eta \mathbf{j} + \frac{\beta_\perp T^2}{3n^2} \mathbf{h} \times \nabla(n^2/T) - \beta_\perp \nabla_\perp T_e \quad (13)$$

Here two special cases can be mentioned: When $n^2/T = \text{const}$, the z component reduces to $E_0 = (\eta/2) j_z$, as earlier derived by Haines[1]. This result corresponds to an isotropic resistivity $\eta/2$. When $T = \text{const}$, we have instead $E_0 = \eta_\parallel j_\parallel + \eta_\perp j_\perp$, which is the conventional form of Ohm's law with anisotropic resistivity.

4. RADIAL PLASMA PROFILES

To obtain explicit solutions we now restrict the analysis to the specific class of axial current density profiles as defined by

$$j_z(r) = j_0 \left[1 - \left(\frac{r}{a} \right)^\alpha \right] + j_a \quad , \quad j_0 = \frac{I_p}{\pi a^2 \left(\frac{\alpha}{\alpha+2} + g_j \right)} \quad (14)$$

Here α is a positive constant, I_p is the total plasma current, and $j_a = j_z(a) \neq 0$ when the plasma core is surrounded by a partially ionized current-carrying boundary layer. Usually $j_a \ll j_0$.

Integration of the z-component of Eq.(1) yields

$$B_\phi(r) = \frac{\mu_0 j_0 r}{2} \left[1 + g_j - \frac{2}{\alpha+2} \left(\frac{r}{a} \right)^\alpha \right] \quad (15)$$

in which expression $g_j \equiv j_a/j_0$. To obtain the plasma pressure $p(r)$ in our numerical calculations, we integrate the radial component of Eq.(2);

$$p' = - \frac{B_\phi}{\mu_0 r} (r B_\phi)' - \frac{B_z}{\mu_0} B_z' - \rho v_r v_r' \quad (16)$$

directly, including the radial diffusion term. From our numerical results, however, it turns out that although the latter term can be strongly contributing in Eq.(9), its contribution to Eq.(16) is usually negligible. The axial magnetic field profile $B_z(r)$ is obtained from Eq.(9) with the boundary condition $B_z(a) = B_{vac}$ = externally applied axial field. In the absence of Nernst and radial diffusion effects, this is a fully self-consistent scheme.

Our model for the Nernst and radial diffusion terms require profiles of temperature and ion source rate. The temperature profile is modelled by

$$T_e(r) = T_0 \left[1 - \left(\frac{r}{a} \right)^\gamma \right] + T_a \quad (17)$$

with γ as a free parameter, and the density profile $n(r) = p(r) / (2T_e(r))$, required for computing the diffusion term in Eq.(16). The radial diffusion velocity is obtained from Eq.(11), with constant source rate profile q_0 .

5. ANALYTICAL RESULTS

In absence of the Nernst effect and radial diffusion, analytic expressions for the pressure and axial magnetic field profiles can be obtained, demonstrating the influence of anisotropic resistivity. In this Section we will also determine an explicit expression for the pinch radius with the paramagnetic effect included.

5.1 The pressure profile

We introduce the parameter

$$B_0 \equiv \frac{\mu_0 I_p}{2\pi a} \left(\frac{\alpha}{\alpha+2} + g_j \right)^{-1} \equiv B_{\varphi a} \left(\frac{\alpha}{\alpha+2} + g_j \right)^{-1} \quad (18)$$

where $B_{\varphi a} = B_{\varphi}(a)$, and $B_0 = B_{\varphi a}$ for $j_a = 0$ and constant current density profile. We further introduce the dimensionless variable $\rho \equiv r/a$ and the dimensionless functions $b_z(\rho)$, $F(\rho)$ and $G(\rho)$, defined by

$$B_z(\rho) \equiv B_0 b_z(\rho) \quad (19)$$

$$F(\rho) \equiv \rho \left[1 + g_j - \frac{2}{\alpha+2} \rho^\alpha \right] \quad (20)$$

$$G(\rho) \equiv 2 \left(1 + g_j - \rho^\alpha \right) = \frac{1}{\rho} \frac{d}{d\rho} (\rho F) \quad (21)$$

Consequently Eq.(15) has the form

$$B_{\varphi}(\rho) = B_0 F(\rho) \quad (22)$$

and Eq.(9) is rearranged into the dimensionless form

$$\frac{db_z}{d\rho} + \frac{(f-1)FG}{fb_z^2 + F^2} b_z = 0 \quad (23)$$

The pressure balance Eq.(16) can finally be integrated to yield the pressure profile ($p_0 \equiv p(0)$):

$$p(\rho) = p_0 - \frac{B_0^2}{2\mu_0} (b_z^2 - b_{z0}^2) + \frac{B_0^2}{\mu_0} \rho^2 \left[(1+g_j)^2 - 2(1+g_j) \frac{\alpha+4}{(\alpha+2)^2} \rho^\alpha + \frac{1}{(\alpha+1)(\alpha+2)} \rho^{2\alpha} \right] \quad (24)$$

5.2 The plasma radius

From Eq.(24) we derive an expression for the plasma radius. First we define $g_p \equiv p_a/p_0$ where $p_0 = 2n_0T_0$ and $p_a = p(a)$. Also, let $g_z \equiv b_{z0}/b_{za} = B_{z0}/B_{za}$. There results

$$a^2 = \frac{\mu_0 I_p^2}{2\pi^2 p_0} \frac{(1+g_j)^2 - 2(1+g_j)\frac{\alpha+4}{(\alpha+2)^2} + \frac{2}{(\alpha+1)(\alpha+2)}}{(1-g_p)\left(\frac{\alpha}{\alpha+2} + g_j\right)^2 \left[1 + (g_z^2 - 1)\frac{B_{za}^2}{\mu_0 p_0}\right]} \quad (25)$$

This relation shows that the plasma radius decreases with increasing paramagnetism ($g_z > 1$), and increases with increasing diamagnetism ($g_z < 1$). It also demonstrates that finite plasma edge pressure ($g_p > 0$) tends to increase the plasma radius. We now raise the following questions: how large is the paramagnetic effect due to anisotropic resistivity and what is its impact on the plasma radius?

5.3 The paramagnetic field

It is far from trivial to obtain analytic solutions to Eq.(9), even for a simple magnetic field profile of the form (15). One exception is provided by the special case of a constant current density profile, for which $\alpha = \infty$. Restricting ourselves to $j_a = 0$ and $f = 2$, Eq.(9) reduces to

$$\frac{dB_z^3}{dr} + \frac{3B_0^2}{2a^2} \frac{d}{dr} (r^2 B_z) = 0 \quad (26)$$

which is integrated to

$$B_z(r) = \left\{ \left[C_1 + \frac{B_0^6}{8} \left(\frac{r}{a} \right)^6 \right]^{1/2} + C_1 \right\}^{1/3} - \left\{ \left[C_1 + \frac{B_0^6}{8} \left(\frac{r}{a} \right)^6 \right]^{1/2} - C_1 \right\}^{1/3} \quad (27)$$

where

$$C_1 = \frac{B_{za}^3}{2} + \frac{3}{4} B_0^2 B_{za} \quad (28)$$

For $r = 0$ we thus obtain from Eq.(27)

$$g_z = \frac{B_{z0}}{B_{za}} = \left[1 + \frac{3B_0^2}{2B_{za}^2} \right]^{1/3}, \quad B_{za} \neq 0 \quad (29)$$

Experimental values of the boundary magnetic fields can be used in this expression to estimate the paramagnetic effect. Using Eq.(29) in Eq.(25) will then also give an estimate of the experimental pinch radius, provided that the on-axis pressure is known, e.g. by Thomson scattering measurements.

The paramagnetic behaviour of the plasma radius in the case of constant current density, with $g_p = g_j = 0$, can further be studied by rewriting Eq.(25) as

$$X \left\{ 1 - \frac{1}{2X} \left[\left(1 + \frac{3}{4}X \right)^{2/3} - 1 \right] \right\} = \beta_a \quad (30)$$

where

$$X \equiv \frac{B_0^2}{B_{za}^2}, \quad \beta_a \equiv \frac{\mu_0 p_0}{2B_{za}^2} \quad (31)$$

For small applied fields B_{za} and large values of X and β_a , Eq.(30) reduces to

$$\frac{\beta_a}{X} = \left(\frac{a}{a_0} \right)^2 = 1 - \left(\frac{3}{4} \right)^{2/3} / (2X^{1/3}) \quad (32)$$

where

$$a_0 \equiv \sqrt{\frac{\mu_0 I_p^2}{2\pi^2 p_0}} \quad (33)$$

is the pinch radius in absence of an imposed field B_{za} . For strong applied fields B_{za} and small values of X and β_a , Eq.(30) reduces instead to

$$\frac{\beta_a}{X} = \left(\frac{a}{a_0} \right)^2 = \frac{3}{4}. \quad (34)$$

As a numerical example we put $I_p = 5 \cdot 10^4$ kA and $p_0 = 8 \cdot 10^4$ Pa, yielding a pinch radius $a_0 = 0.0446$ m in absence of an imposed axial field. When imposing the axial field $B_{za} = 0.2$ T, the pinch radius reduces to $a = 0.0388$ m according to Eq.(30), i.e. it shrinks by about 11 percent.

6. NUMERICAL RESULTS

The radial variation of the axial magnetic field $B_z(r)$ due to resistivity anisotropy is shown in Fig.1. We have chosen parameters close to those of the toroidal Extrap-T1 experiments. Clearly, the strongest paramagnetic effect appears at peaked current density and high kinetic pressure; as the current density becomes more peaked, the innermost field lines become more twisted in the poloidal direction. This naturally causes an enhancement of the center axial magnetic field, i.e. paramagnetism. Our Eq.(29), which gives $g_z = B_{z0}/B_{za}$ for constant current density, is verified in Fig1.b). Judging from Fig.1a), Eq.(29) gives a good estimate of paramagnetism also for a current profile with $\alpha = 2$. Note that the relative paramagnetic effect increases with decreasing B_{za} . In Fig.1c) we show a case where radial particle diffusion is strong enough to cause a marginally diamagnetic effect at high B_z .

Paramagnetism decreases the equilibrium plasma radius. It is shown in Fig.2 (with the same parameters as in Fig. 1) that this effect is strong for relatively weak fields B_z . The fact that the radius is smaller for constant current density (Fig.2b) than for peaked current density (Fig.2a), which gives enhanced paramagnetism, is somewhat astonishing at first but consistent with Eq.(25). Note from Eq.(9) that, in absence of radial particle flow, Fig.2 can be quite universally applied; the plasma radius scales linearly with total plasma current I_p . Also, the figure can be extended to larger values of $B_z(a)$; the plasma radius is approximately constant for large values of $B_z(a)$, according to Eqs.(25) and (29).

The Nernst term gives a diamagnetic effect, and increasing plasma radius, for the parameters in Fig.2 at high pressure. This is particularly clear in Fig.2 c), where we have artificially set $f = 1$ to see the effect of the Nernst term alone. The reason for the diamagnetic effect is that, for fixed temperature, the density increases with increasing pressure. Inevitably, the ratio of the Nernst term to ideal terms, as given in Eq. (10), goes up. The Nernst effect will be small in a reactor due to its high temperature plasma.

In Fig.2 d) we show a case, where radial particle diffusion is large enough to cause a significant diamagnetic effect. For given ion source rate, this effect becomes pronounced at small ion pressures p , since then the ratio of neutrals to ions n_n/n is large; see discussion in Section 3. It is clear that radial particle diffusion, through e.g. pellet injection, can contribute a large current. This is an important means for steady state current drive in any screw pinch.

Extrap was originally conceived as a Z-pinch. The last few years it has been realized that both the linear L1 version and the toroidal T1 version can be run in ultra-low q (ULQ) modes, i.e. configurations where the safety factor on edge, $q(a)$, is less than unity. As we will see in later figures, this is one of at least two ways to go to achieve high beta (>10%) in a device with axial magnetic field; the Kruskal-Shafranov limit $q(a) > 1$ is unacceptable for obtaining high beta. A second alternative is of course the RFP.

In Fig.3 a) parameters for Extrap-L1 are used. This device features a relatively sharp $q(a) > 1/2$ limit, above which current is lost from inside the separatrix. Regarding this as a stability limit, we see from Fig.3a) that the operational window becomes quite small. The radii of equilibria, obeying $q(a) > 1/2$, are forced towards and past the separatrix and against material supports. This causes current to flow outside the separatrix; the $q(a) > 1/2$ limit implies lack of equilibrium. We add that the separatrix in Extrap is created by four parallel external rod currents, flowing anti-parallel to the plasma current. The separatrix distance is a weak function of the ratio between plasma and rod currents.

Now study Fig.3b), where parameters characteristic for ULQ modes in the toroidal Extrap-T1 Upgrade device are used. Obviously equilibria confined inside the separatrix shown in the figure cannot be achieved unless the stability limit is lowered to values of $q(a) < 1/2$, no matter what pressure p_0 is assumed. The separatrix, limiting the plasma radius, can in reality only be marginally increased since the vacuum vessel, with an inner wall distance of 0.057 m, is placed inside the octupole field coils in this device. In conclusion, to avoid plasma 'resting against the wall', very high axial magnetic fields and an optimized separatrix, situated near the wall, must be used for $q(a) > 1/2$ operation with sufficiently high current in Extrap T-1.

Equilibrium plasma radii for reactor-like parameters are given in Fig.4. Nernst diamagnetism is negligible here. This computation was primarily done for calculations of reactor plasma beta β_{av} , which are shown in Figs. 5 and 6.

Let us for a moment discuss the definition of and dependence in β_{av} . A physically convenient definition is

$$\beta_{av} \equiv \frac{2\mu_0 \langle p \rangle}{\langle B^2 \rangle} \quad (35)$$

since it can be used for comparisons of any fusion-related magnetic confinement scheme[8]. Here $\langle \dots \rangle$ denotes surface average. Assuming $B_z(r) = \text{constant}$ and vanishing edge pressure, the Bennett relation implies $\langle p \rangle = B_p^2(a)/(2\mu_0)$. Constant current density further gives $\langle B^2 \rangle = B_z^2(a) + B_p^2(a)/2$. Finally defining $q(a) \equiv aB_z(a)/(RB_p(a))$, we obtain

$$\beta_{av} \approx \frac{1}{\left(\frac{R}{a}\right)^2 q^2(a) + \frac{1}{2}} \quad (36)$$

When paramagnetism is included, $\langle p \rangle$ decreases and $\langle B^2 \rangle$ increases, and the above estimate becomes an upper bound for β_{av} . Since a peaked current density profile yields a higher value of $\langle B^2 \rangle$, Eq.(36) remains a valid estimate of the maximum obtainable β_{av} .

In Figs.5 and 6 we show computed values of β_{av} for the reactor parameters of Fig.4. A realistic reactor aspect ratio of $R/a = 4$ has been used. We have included the effect of paramagnetism due to anisotropic resistivity in these figures. Clearly, our computed plasma beta values are smaller than those given by Eq.(36). We have neglected toroidal effects, but it does not seem reasonable that plasma and profile shaping could raise β_{av} to values acceptable for the D-D reaction for values of $q(a) > 1/2$.

Finally we have computed values of β_{av} for the parameters of Fig.2 a) in Figs. 5 and 6. An aspect ratio $R/a = 8$ is here assumed. Knowledge of p_0 , i.e. of on-axis temperature and density are again required to estimate β_{av} from the figures. Note that β_{av} is profile-dependent, hence does not necessarily equal unity. Further, we have assumed $p_a/p_0=0.05$ throughout, which raises β_{av} slightly.

7. CONCLUSIONS

This is a study of paramagnetic and diamagnetic effects on a cylindrical plasma. The force balance and the generalized Ohm's law have been used in combination with Maxwell's equations. For given equilibrium profiles, the equilibrium plasma radius then becomes completely defined, and is found to be sensitive on the dominating mechanism. Anisotropic resistivity always causes a paramagnetic effect and a reduction of the pinch radius. This effect sometimes competes with the diamagnetic Nernst effect (the current across the magnetic field due to temperature gradients) and with the diamagnetic effect due to radial diffusion of ions, which tend to increase the radius.

Our basic result is a relation which determines the radial variation of the axial magnetic field $B_z(r)$, with the above effects included. Further, our model is self-consistent when the diamagnetic effects are negligible. This is usually the case for reactor-like conditions, for which we find that the average plasma beta given by the usual poor scaling $\beta_{av} \approx [(R/a)q(a)]^{-2}$ is decreased further. Hence operation below the Kruskal-Shafranov limit $q(a) > 1$ becomes absolutely necessary for D-D scenarios. Plasma and profile shaping is not enough, and the aspect ratio R/a should be kept at a value of about four, for engineering reasons.

We have also found that there can be a conflict between stability limits which require large values of the edge safety factor $q(a)$ and between equilibrium requirements. In order to obtain sufficiently high $q(a)$, the equilibrium plasma radius is pushed outside the magnetic or material limiters, and a loss of confinement results. Plasma temperature and density should be determined to ensure that the plasma pressure falls within the possible range of operation, according to Fig.3. Very narrow possible regimes of operation results even for ULQ operation with $q(a) > 1/2$ in present Extrap-L1 and T1 Upgrade devices, unless the axial magnetic field $B_z(a)$ can be increased further.

The coupling between the transverse (poloidal) and axial (toroidal) magnetic field components in the presence of an externally applied axial field, as described here, is basically different to the Taylor relaxation mechanism. We investigate a general effect caused by anisotropic resistivity, whereas the Taylor mechanism can only be triggered in certain geometries, like in the reversed field-Pinch.

A problem with the present analysis is that experimental resistivity is not classical. In Extrap discharges e.g., the measured resistivity in absence of axial field is more than a factor 10 larger than classical. The anomaly factor decreases with increasing axial field, but is still substantial. Our results are fortunately independent of the magnitude of the resistivity, however dependent on the anisotropy ratio f . We have used the classical, collisionality dependent Braginskii transport coefficients throughout.

ACKNOWLEDGEMENT

We would like to thank Professor Malcolm Haines for suggesting to us to reconsider the Nernst term in Ohm's law.

REFERENCES

- [1] Haines, M.G., *Plasma Phys. Contr. Fusion* **28**(1986)1705.
- [2] Lehnert, B., *Physica Scripta* **12**(1975)327.
- [3] Bodin, H.A.B., *Nuclear Fusion* **30**(1990)1717.
- [4] Taylor, J.B., in **Pulsed High Beta Plasmas**, Proc. Third Top. Conf., Abingdon (1975), Pergamon Press, London 1976, p. 59.
- [5] Lehnert, B., *Fusion Technology* **16**(1989)7.
- [6] Brunzell, P., Hellblom, G., Karlsson, P., Mazur, S., Nordlund, P., and Scheffel, J., **Controlled Fusion and Plasma Heating** (Proc. of 17th European Conf. Amsterdam 1990), **14B**, Part II(1990)610.
- [7] Epperlein, E.M. and Haines, M.G., *Phys. Fluids* **29**(1986)1029.
- [8] Green, B.J., Jacquinot, J., Lackner, K. and Gibson, A., *Nucl. Fusion* **16**(1976)521.

FIGURE CAPTIONS

- Fig.1** Radial profiles of the axial magnetic field $B_z(r)$; units in m and T.
- Paramagnetic effect for peaked current density profile. No radial particle diffusion. Parameters: $I_p = 10\text{kA}$, $\alpha = 2$, $E_0 = 100\text{V/m}$, $p_0 = 10^3\text{ Pa}$, $p_a/p_0 = 0.05$, $T_0 = 30\text{eV}$, $T_a/T_0 = 0.1$, $\gamma = 2$, $q_0 = 0$, f given by Braginskii.
 - As in a), except that the current density profile is flat; $\alpha = 100$.
 - As in a), except that a diamagnetic effect due to radial particle diffusion is present; $q_0 = 2 \cdot 10^{23}\text{ m}^{-3}\text{s}^{-1}$.
 - As in a), except that the kinetic pressure is higher; $p_0 = 10^4$.
- Fig.2** Equilibrium plasma radius a as function of boundary axial magnetic field $B_z(a)$ for different on-axis pressures p_0 .
- Parameters as in Fig.1 a); peaked current density profile.
 - Case corresponding to Fig.1 b).
 - As in Fig.1 a), except that resistivity is assumed isotropic; $f = 1$.
 - Case corresponding to Fig.1 c).
- Fig.3** Equilibrium plasma radius a as function of boundary axial magnetic field $B_z(a)$ for different on-axis pressures p_0 . The average separatrix distance for equal external rod and plasma currents and the $q(a) = 1/2$ limit are indicated. f is given by Braginskii.
- Parameters for the linear Extrap-L1 experiment in Stockholm:
 $I_p = 5\text{kA}$, $\alpha = 2$, $E_0 = 5\text{kV/m}$, $p_a/p_0 = 0.05$, $T_0 = 20\text{eV}$, $T_a/T_0 = 0.1$, $\gamma = 2$, $q_0 = 0$.
 - Parameters for the toroidal Extrap-T1 Upgrade experiment in Stockholm:
 $I_p = 15\text{kA}$, $\alpha = 2$, $E_0 = 100\text{V/m}$, $p_a/p_0 = 0.05$, $T_0 = 20\text{eV}$, $T_a/T_0 = 0.1$, $\gamma = 2$, $q_0 = 0$.
- Fig.4** Equilibrium plasma radius a as function of boundary axial magnetic field $B_z(a)$ for different on-axis pressures p_0 . Tokamak reactor-like parameters are used:
 $I_p = 10\text{MA}$, $\alpha = 2$, $E_0 = 0.05\text{V/m}$, $p_a/p_0 = 0.05$, $T_0 = 10\text{keV}$, $T_a/T_0 = 0.1$, $\gamma = 2$, $q_0 = 0$, f given by Braginskii.
- Fig.5** Average plasma beta β_{av} as function of boundary axial magnetic field $B_z(a)$ for different on-axis pressures p_0 .
- Corresponding to case in Fig.2 a).
 - Corresponding to reactor case of Fig.4.
- Fig.6** Average plasma beta β_{av} as function of boundary safety factor $q(a)$ for different on-axis pressures p_0 .
- Corresponding to case in Fig.2 a). Aspect ratio $R/a = 8$.
 - Corresponding to reactor case of Fig.4. Aspect ratio $R/a = 4$.

Fig. 1

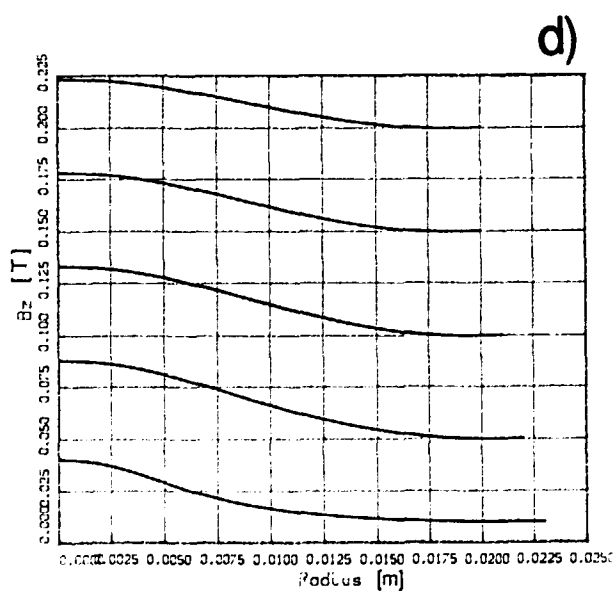
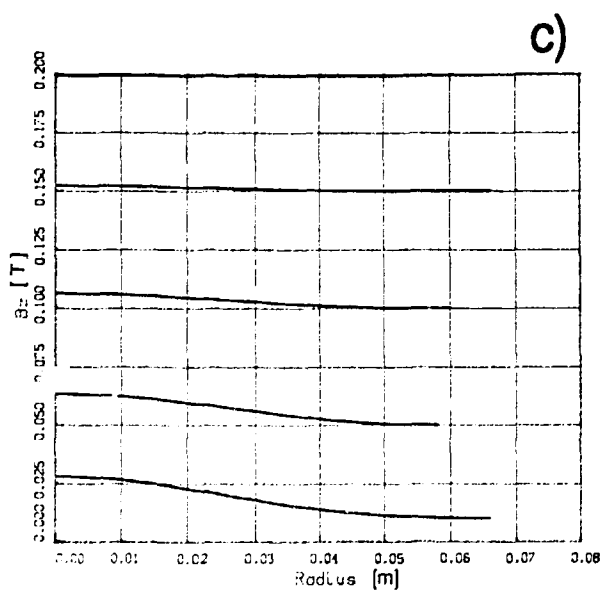
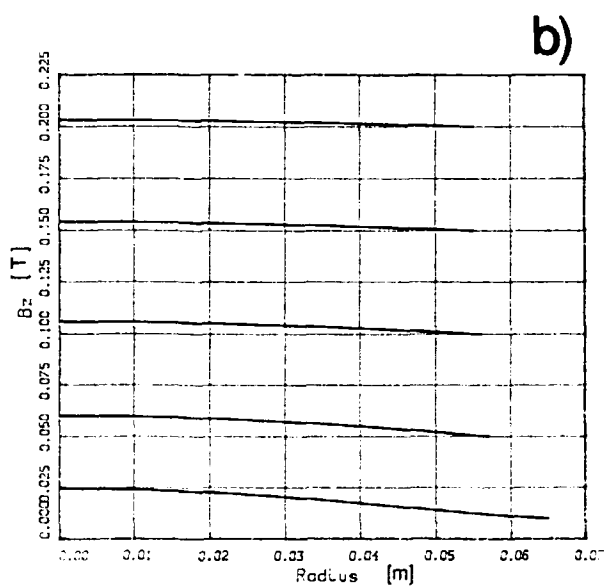
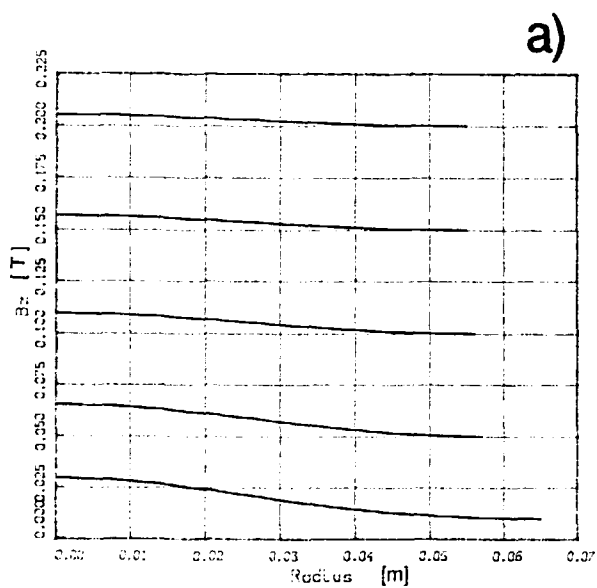


Fig.2

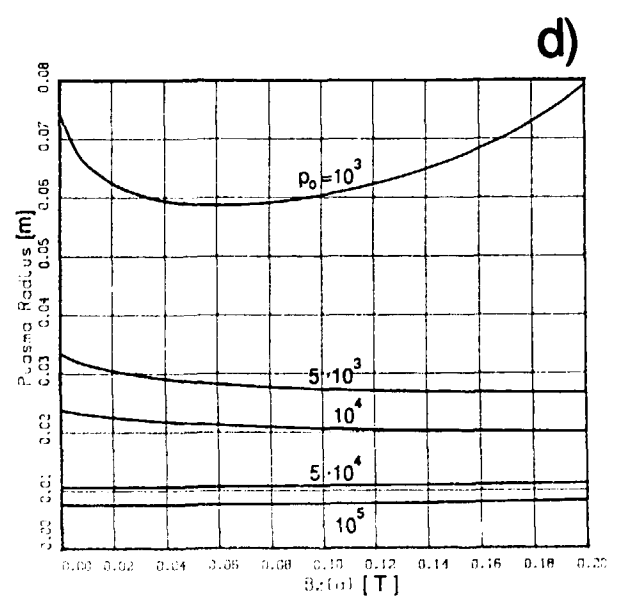
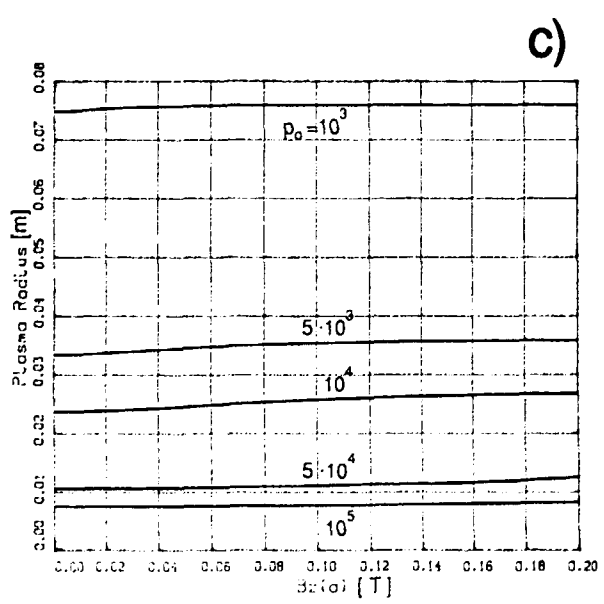
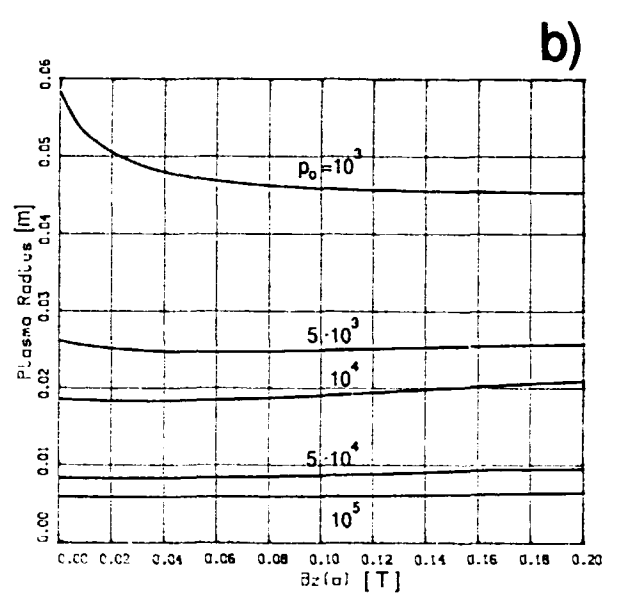
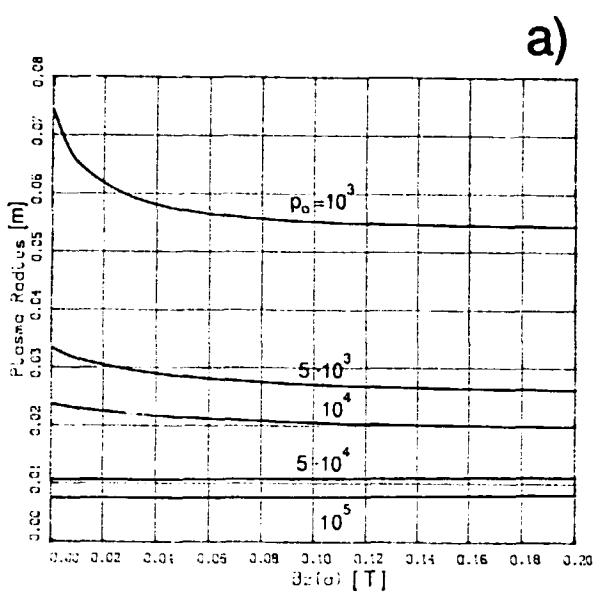


Fig.3

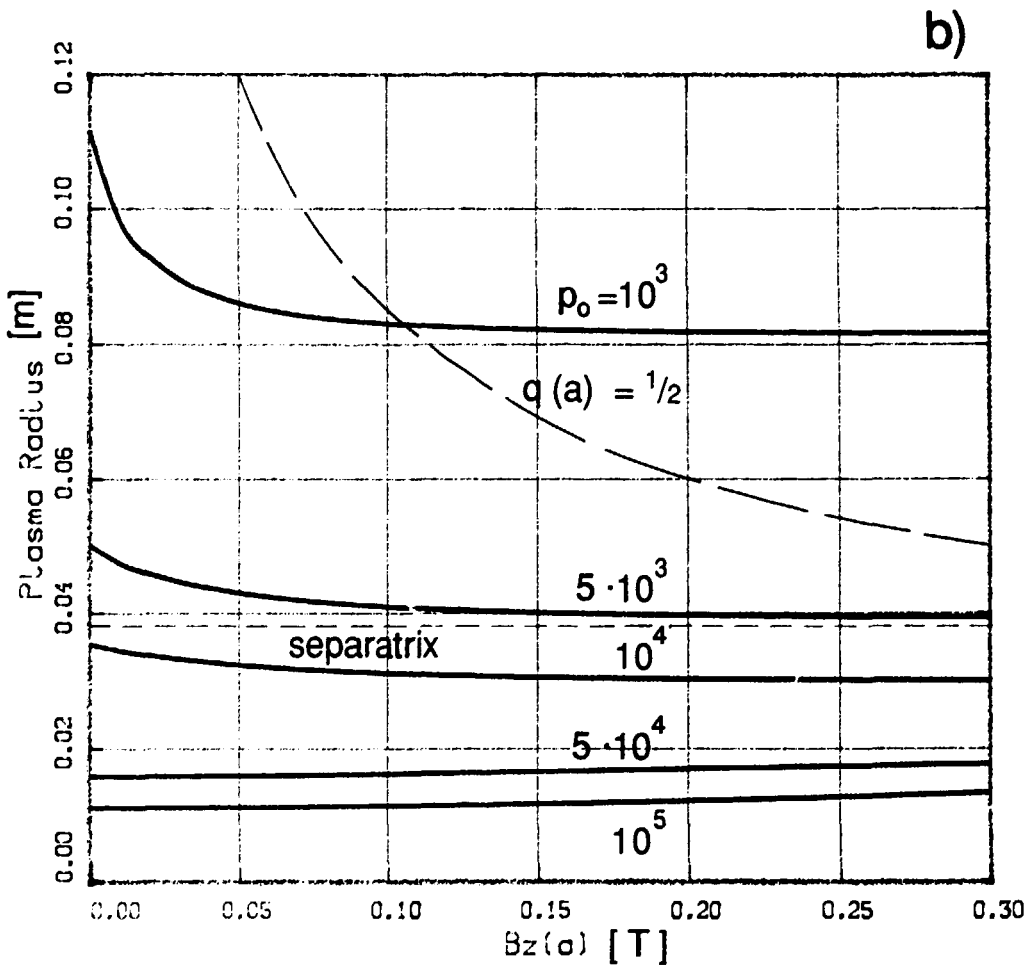
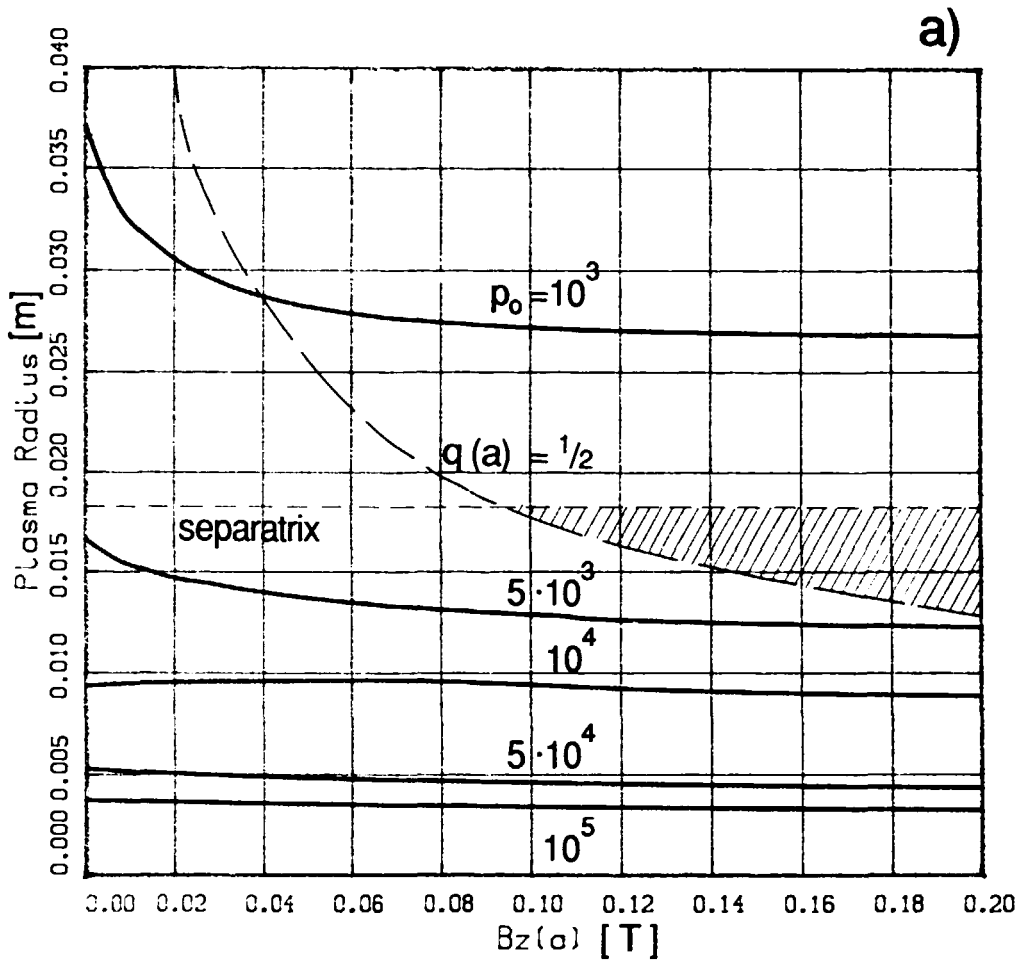


Fig.4

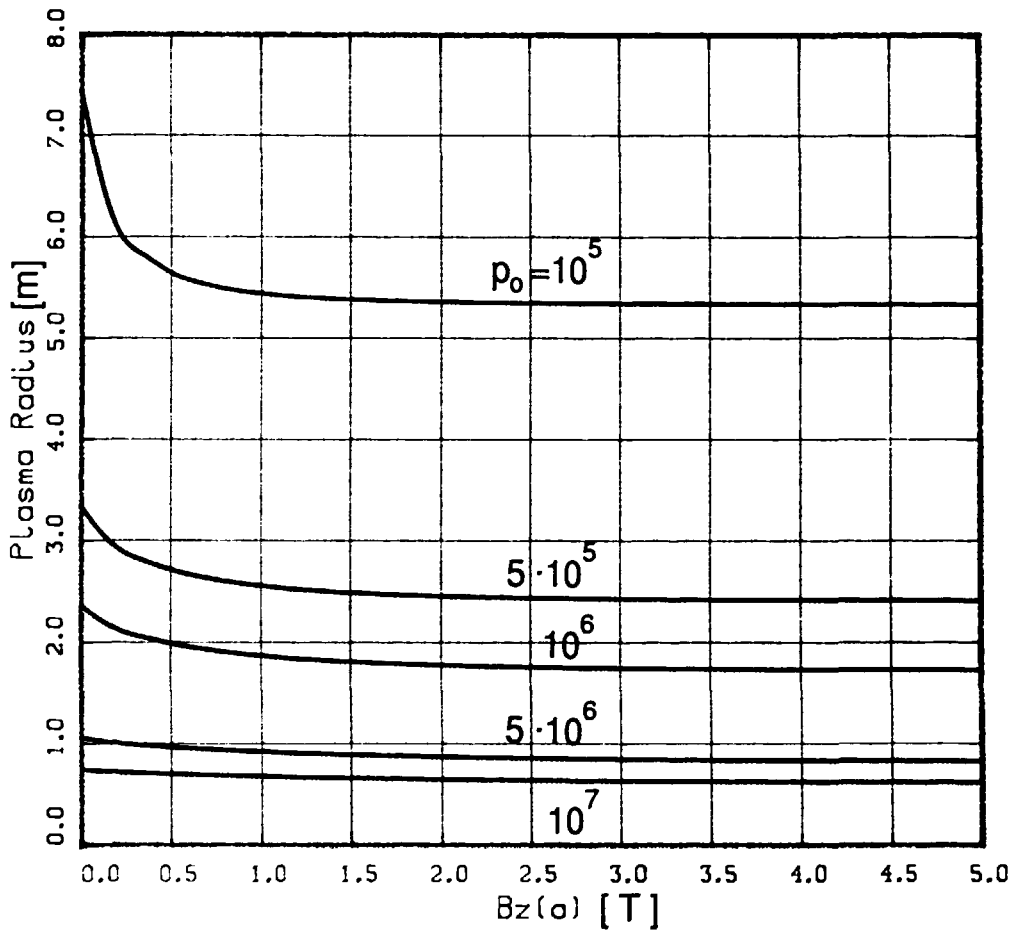


Fig.5

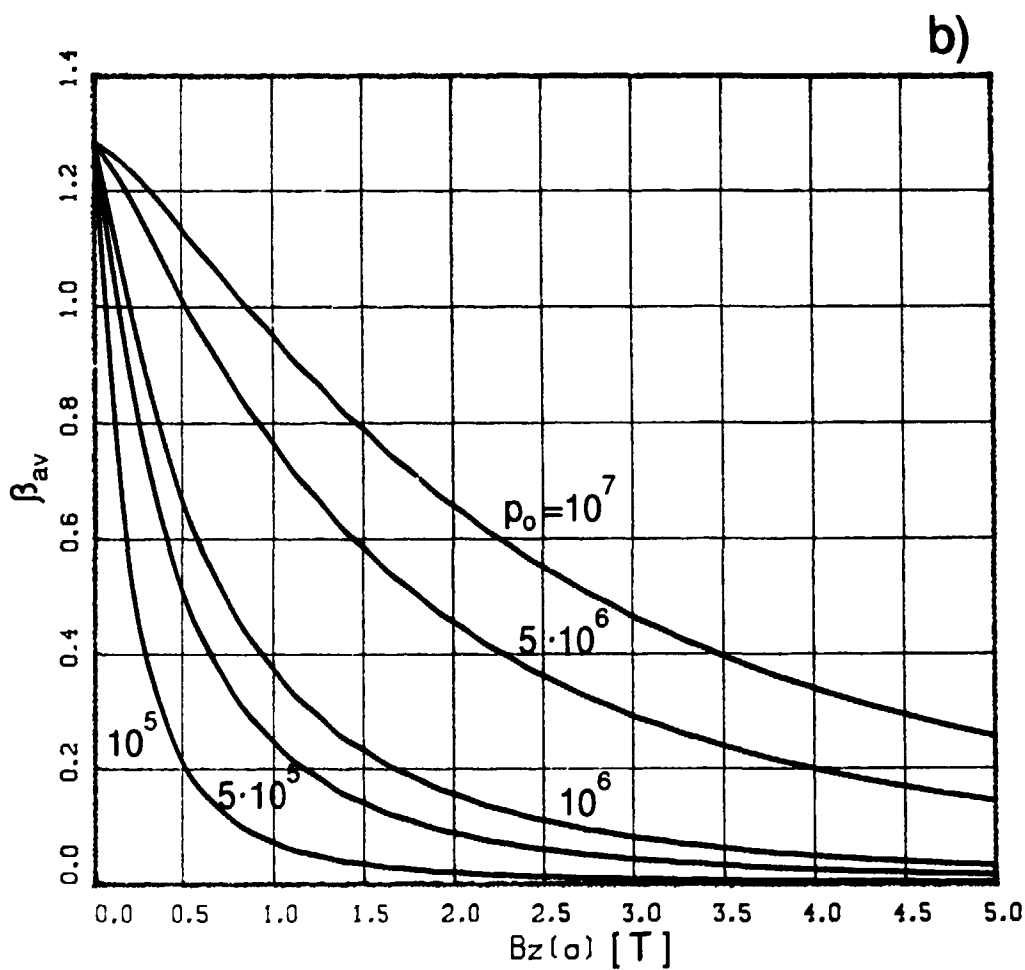
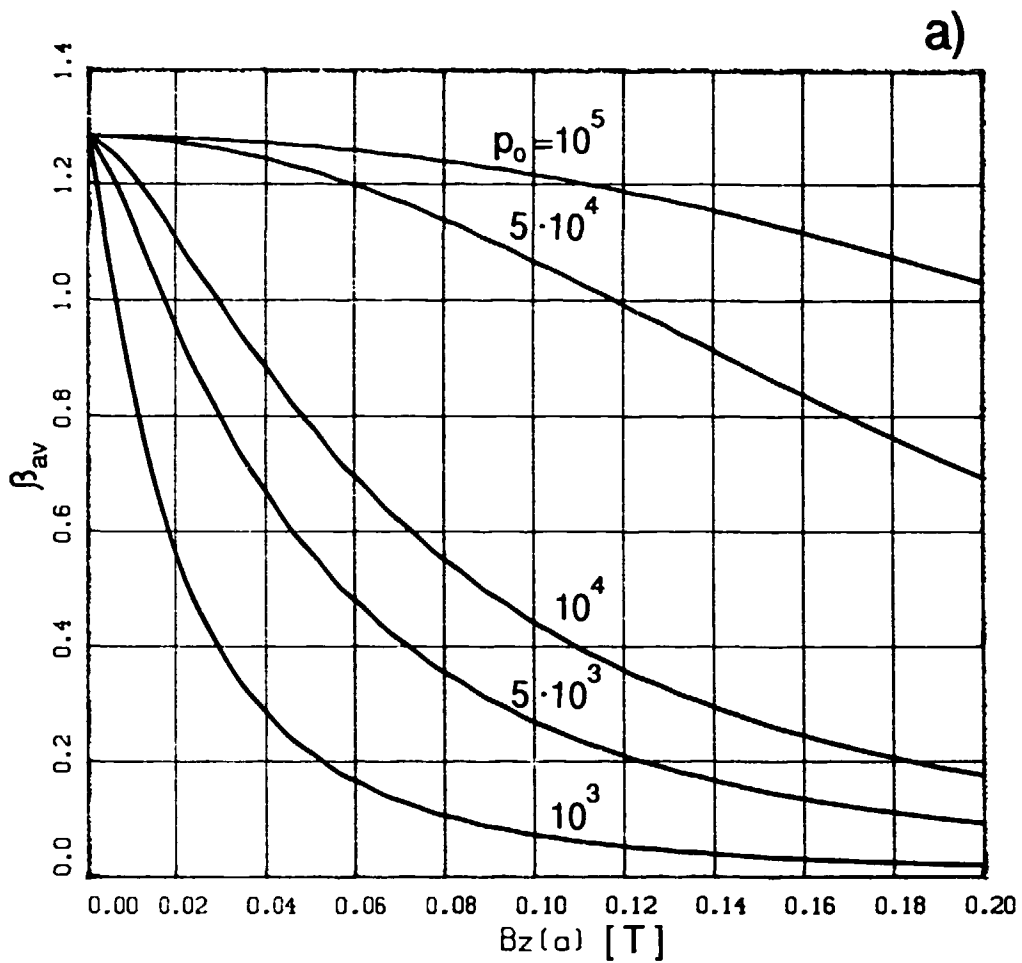
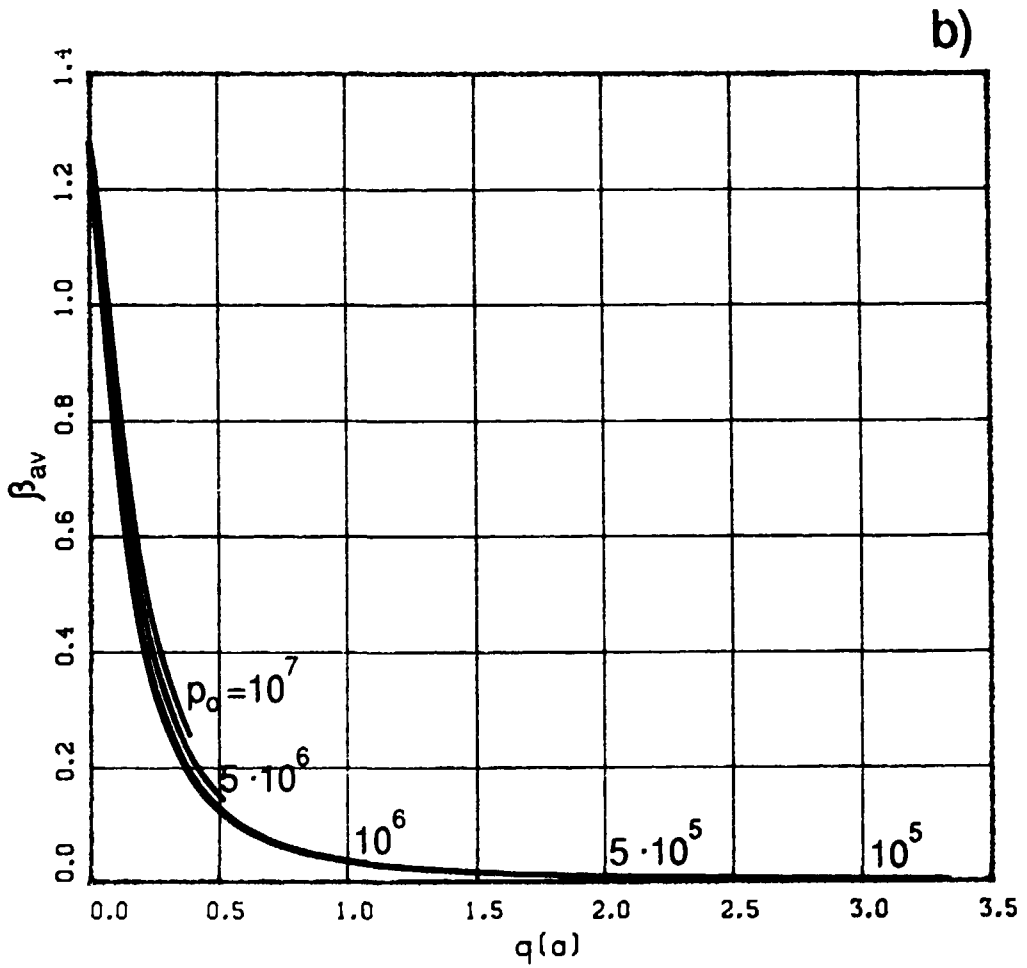
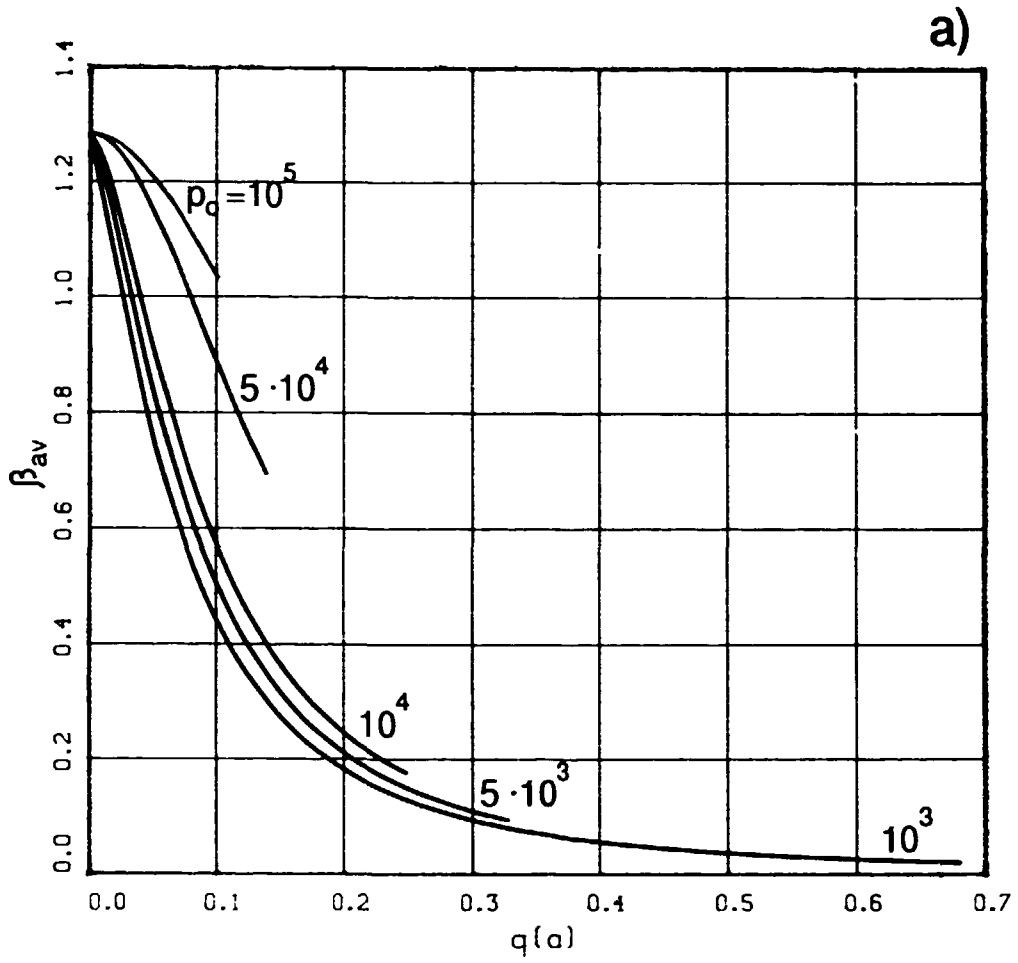


Fig.6



TRITA-PFU-91-03

Department of Plasma Physics and Fusion Research,
Alfvén Laboratory, Royal Institute of Technology, S-100 44 Stockholm, Sweden

PARAMAGNETISM AND PLASMA BETA IN A SCREW-PINCH

B. Lehnert and J. Scheffel, 24p. incl. figs, in English.

Anisotropic resistivity causes paramagnetic effects ($B_z'(r) < 0$) in a screw pinch, being basically different to the self-relaxation described by Taylor. We compute, analytically and numerically, the resulting effect on equilibrium in a 1-D straight cylindrical plasma. In particular we compute paramagnetic effects on the plasma radius and on plasma beta. Ohm's law also contains diamagnetic terms; in this paper we consider radial particle diffusion and the Nernst effect. In a Tokamak or reactor plasma these effects are shown to be negligible, whereas they may contribute in present ULQ, Extrap and RFP experiments.

A basic result is an expression for the coupling between the poloidal and axial magnetic field components with the above effects included. A result of specific importance to the Extrap programme is that plasma current limitation can arise from lack of equilibrium when the plasma radius tends to exceed its upper limit, being defined by a magnetic or material limiter. The paramagnetic effect described in this work lower plasma beta further, making D-D reactors depending on safety factors $q(a) > 1$ seem less attainable.

Key words: Extrap, ULQ, paramagnetism, diamagnetism, beta value, safety factor.